Injectable Self-Healing Glucose-Responsive Hydrogels with pH-Regulated Mechanical Properties

Citation: Yesilyurt, Volkan et al. "Injectable Self-Healing Glucose-Responsive Hydrogels with pH-Regulated Mechanical Properties." Advanced Materials 28.1 (2016): 86–91.

As Published: http://dx.doi.org/10.1002/adma.201502902

Publisher: Wiley Blackwell

Persistent URL: http://hdl.handle.net/1721.1/107195

Version: Original manuscript: author's manuscript prior to formal peer review

HHS Public Access

Author manuscript

Adv Mater. Author manuscript; available in PMC 2016 April 08.

Published in final edited form as:

Adv Mater. 2016 January ; 28(1): 86–91. doi:10.1002/adma.201502902.

Injectable Self-Healing Glucose-Responsive Hydrogels with pH-Regulated Mechanical Properties

Volkan Yesilyurt,
David H. Koch Institute for Integrative Cancer Research Massachusetts Institute of Technology, Cambridge, MA 02139, USA

Department of Anesthesiology, Boston Children's Hospital, Boston, MA 02115, USA

Matthew J. Webber,
David H. Koch Institute for Integrative Cancer Research Massachusetts Institute of Technology, Cambridge, MA 02139, USA

Department of Anesthesiology, Boston Children's Hospital, Boston, MA 02115, USA

Eric A. Appel,
David H. Koch Institute for Integrative Cancer Research Massachusetts Institute of Technology, Cambridge, MA 02139, USA

Colin Godwin,
Department of Chemical Engineering, Massachusetts Institute of Technology, Cambridge, MA 02139, USA

Robert Langer, and
David H. Koch Institute for Integrative Cancer Research Massachusetts Institute of Technology, Cambridge, MA 02139, USA

Department of Anesthesiology, Boston Children's Hospital, Boston, MA 02115, USA

Department of Chemical Engineering, Massachusetts Institute of Technology, Cambridge, MA 02139, USA

Harvard–Massachusetts Institute of Technology Division of Health Sciences and Technology, Institute for Medical Engineering and Science, Massachusetts Institute of Technology, Cambridge, MA 02139, USA

Daniel G. Anderson
David H. Koch Institute for Integrative Cancer Research Massachusetts Institute of Technology, Cambridge, MA 02139, USA

Department of Anesthesiology, Boston Children's Hospital, Boston, MA 02115, USA

Department of Chemical Engineering, Massachusetts Institute of Technology, Cambridge, MA 02139, USA

Correspondence to: Daniel G. Anderson, dgander@mit.edu.

Supporting Information

Supporting Information is available from the Wiley Online Library or from the author.

Harvard–Massachusetts Institute of Technology Division of Health Sciences and Technology, Institute for Medical Engineering and Science, Massachusetts Institute of Technology, Cambridge, MA 02139, USA

Daniel G. Anderson: dgander@mit.edu

Hydrogels are an appealing class of materials for many biomedical applications, ranging from tissue engineering to drug delivery, and offer a number of functional benefits as a result of their high water content and solid-like mechanical properties. [1–3] Typically, hydrogels are prepared from either covalent or physical cross-linking of hydrophilic polymers to form an insoluble network. Covalently cross-linked hydrogels are typically mechanically stable and elastic, but lack shear-thinning and self-healing properties that are required for applications necessitating minimally invasive injection or catheter delivery. Hydrogels physically cross-linked through ionic interactions, in general, exhibit reduced mechanical properties and are less stable than those produced through covalent cross-linking. Imparting hydrogels with mechanical properties that can be responsive to biologically relevant environmental stimuli could also be of broad interest for biomedical applications. [4,5] The use of dynamic covalent chemistry offers an attractive route in order to prepare hydrogels that could exhibit shear-thinning and self-healing characteristics. These materials would leverage cross-linking mechanisms that arise from a number of recently reported dynamic covalent chemistries. [6–9] One example would be to form hydrogel materials by using the complexation of boronic acids and *cis*-1,2 or *cis*-1,3 diol compounds as cross-links in the material. [10–13] The formation of diol–boronic acid complex occurs at pH greater than or equal to the pK_a of the boronic acid, and since most boronic acids used to prepare materials through this cross-linking mechanism have pK_a values of ≥8 these materials have limited utility in physiologic conditions. [14,15] The pH sensitivity of this dynamic covalent bond does introduce the ability to form dynamically restructuring hydrogels with mechanical properties that are responsive to changes in pH.

Here, we report on the design, synthesis, and application of poly(ethylene glycol) (PEG)-based shear-thinning and self-healing hydrogel networks prepared using reversible covalent interactions between phenylboronic acid (PBA) derivatives and *cis*-diols. The dependence of gel strength on pH was systematically studied using nine hydrogel formulations composed of PBA derivatives with varied pK_a. These materials were further evaluated for use in the delivery of protein therapeutics as well as three-dimensional (3D) cell culture substrates, and biocompatibility was assessed following subcutaneous syringe injection.

PEG macromonomers containing either PBA groups or a glucose-like diol (Figure 1) were constructed by modifying four-arm PEG-NH_2 (5 kDa) with various phenylboronic acid derivatives. PEG-NH_2 was functionalized using HBTU-activated 4-carboxy-3-fluorophenylboronic acid or 4-carboxyphenylboronic acid to yield PEG-FPBA and PEG-PBA, respectively. Alternatively, 2-formylphenylboronic acid was coupled via reductive amination with PEG-NH_2 to yield PEG-APBA. The pK_a of these three phenylboronic acid groups have been reported in literature and are ranked as PBA (7.8) > FPBA (7.2) > APBA (6.5–6.7). [16–18] To prepare a macromonomer containing a glucose-like diol, D-glucolactone was reacted with PEG-NH_2 in the presence of triethylamine to yield PEG-diol.

The products were dialyzed and lyophilized to yield a white powder. All PEG derivatives exhibited water solubility of up to 40 w/v% in various buffers. Detailed information on synthesis and characterization of macromolecules can be found in the Supporting Information.

An array of nine hydrogels was formulated by mixing each of the PEG-phenylboronic acid macromonomers with equimolar PEG-diol macromonomer in three different pH buffers (pH 6–8). All formulations resulted in rapid gel formation (within 10–30 s), with the exception of PEG-PBA, which did not gel at pH 6 likely because this particular phenylboronic acid has a higher pK_a than the others evaluated. We hypothesized that gels should become weaker when pH is below the pK_a of the phenylboronic acid conjugated to the PEG macromonomer. Thus, it was expected that hydrogels formed from PEG-APBA would exhibit the strongest mechanical properties across the range of pH evaluated, since this phenylboronic acid had the lowest pK_a value of three used here. Initially, oscillatory strain sweeps were run to determine the linear viscoelastic region for these hydrogels. Then, dynamic frequency sweep measurements were performed within the viscoelastic region to determine the crossover frequency (ω_c) in order to quantify the gel strength. In a frequency sweep, ω_c is the frequency at which the elastic modulus G' (storage modulus) is equal to the viscous modulus G'' (loss modulus). In hydrogels with lower ω_c, the mechanical properties are dominated by the storage modulus over a broader frequency range, resulting in more elastic behavior and higher strength. [19] As seen in Figure 2a–c, PEG hydrogels prepared from cross-linking phenylboronic acid with glucose-like diols demonstrated frequency-dependent viscoelastic behavior in all pH conditions, a typical behavior of dynamic gel networks. [20–22] At low frequencies, G'' was greater than G', indicating liquid-like character. However, at higher frequencies, G' was greater than G'', indicating gel-like character. As predicted, ω_c correlated with the rank of pK_a values for the three phenylboronic acids, with the lowest pKa PEG-APBA having the smallest ω_c across the pH range tested and the highest pK_a PEG-PBA having the largest ω_c (Figure 2d). In addition, all phenylboronic acid gels demonstrated pH dependence, with ω_c decreasing as pH is increased. For example, ω_c of the PEG-FPBA hydrogel was 22 rad s^{-1} at pH 6, 12 rad s^{-1} at pH 7, and 4 rad s^{-1} at pH 8. Comparatively, at pH 7 the ω_c for PEG-APBA gels was 1.2 rad s^{-1}, indicating stronger gel formation when compared to PEG-FPBA at the same pH. This is likely attributable to the lower pK_a of phenylboronic acid used for PEG-APBA. Thus, the relationship between pK_a of the phenylboronic acid and the environmental pH dictates the extent of cross-linking in these hydrogels. Compared to the other hydrogels, the PEG-APBA was quite rigid and difficult to mold or inject at pH 6–8, likely due to a highly cross-linked network. PEG-FPBA at all pH values, PEG-PBA at pH 7 and pH 8 produced hydrogels that were soft, moldable, and which could be injected through a standard syringe needles (i.e., 21 G).

Next, we studied the shear-thinning and self-healing properties of these hydrogels. We selected the gels formed at pH 7 for the following studies as this pH is more relevant to physiological conditions. Gel formation occurs as a result of dynamic formation of boronic esters between phenylboronic acid and *cis*-diol, and the reversible and dynamic nature of this interaction should translate to dynamic mechanical properties. First, the effect of high shear rates on gel viscosity, a critical parameter for injectability, was measured. As expected, the viscosity of 10 w/v% PEG-FPBA and PEG-PBA gels at 37 °C decreased with increasing

shear rates (Figure 3a and Figure S1a, Supporting Information), indicating a shear-thinning behavior as dynamic cross-links in the gel network are disrupted by shear. This behavior was visualized by injecting 10 w/v% PEG-FPBA gel through 21 G needle (Figure 3a, inset). We were not able to conduct flow experiments on PEG-APBA hydrogels at pH 7 because under high shear this gel breaks apart and is expelled from the cone-disk rheometer. This is most likely due to the highly rigid and brittle character of the PEG-APBA gel, which in essence behaves more like a typical covalently cross-linked hydrogel network that does not exhibit shear-thinning and self-healing properties.

An injectable hydrogel designed for in vivo gelation should undergo structural recovery (self-heal) upon relaxation of the applied stress. To examine self-healing properties, strain-dependent oscillatory measurements were first conducted on 10 w/v% PEG-FPBA hydrogel formed at pH 7 to determine the critical strain value required to disrupt the gel network and transition to a solution state, found here to be 60% (Figure 3b). Step–strain measurements were then performed to determine recovery of hydrogel mechanical properties following network rupture at high strains. For this purpose, 10 w/v% PEG-FPBA and PEG-PBA gels formed at pH 7 were subjected to high strain (γ = 500%) and G' immediately dropped to ≈10 Pa, with the corresponding inversion of G' and G'' indicating network disruption. When high strain was discontinued and a low magnitude strain (γ = 0.05%) was applied, the hydrogel exhibited 100% recovery of both G' and G'' within a few seconds after strain-induced failure, which was reproducible upon additional strain cycles (Figure 3c and Figure S1b, Supporting Information). Additionally, time–sweep experiments immediately after rapid continuous flow (preshearing performed at 100 s^{-1}) was performed using 10 w/v% PEG-FPBA and PEG-PBA gels formed at pH 7 to demonstrate the time frame of healing. There was an immediate recovery of the material properties after high preshear rates were removed (Figure S1c,d, Supporting Information). Furthermore, step–shear measurements, which are conceptually similar to step–strain measurements, whereby one monitors the increase in viscosity at a low magnitude shear rate following high magnitude shear in continuous flow, was performed using the same hydrogel formulations. A high magnitude shear rate (100 s^{-1}) was applied to break down the hydrogel network, followed by a low magnitude shear rate (0.05 s^{-1}) in order to monitor the recovery of bulk material properties (Figure S1e,f, Supporting Information). The observed complete recovery of the viscosity after network destruction supports the self-healing characteristics of 10 w/v% PEG-FPBA and PEG-PBA hydrogels formed at pH 7.

Self-healing of PEG-FPBA gel was also verified by reforming the hydrogel from two pieces (Figure 3d). Healing occurred instantly, and the resultant hydrogel maintained its integrity even upon mechanical agitation with forceps.

Once the hydrogel mechanical properties had been characterized, we examined the potential of these hydrogels for controlled delivery of biomacromolecules as well as for cell encapsulation. These studies focused on PEG-FPBA hydrogel as a result of its ease of injectability compared to PEG-APBA and its better mechanical strength compared to PEG-PBA. Three model proteins, fluorescein isothiocyanate (FITC)-labeled insulin (≈5800 g mol^{-1}), bovine serum albumin-FITC (BSA-FITC) (≈66 000 g mol^{-1}), and Alexa Fluor-conjugated immunoglobulin G (IgG) (≈150 000 g mol^{-1}) were chosen as representative

proteins to span a range of molecular weights. Proteins could be encapsulated within 10 w/v % PEG-FPBA hydrogels by combining them into either of the macromonomer precursor solutions prior to hydrogel formation. Efficient protein incorporation was achieved in all cases with no observable changes to hydrogel properties. The protein-loaded gels were incubated at 37 °C in a phosphate-buffered saline (1× PBS) bulk phase, which was collected at serial time points and quantified using fluorescence spectroscopy. The release profiles for all proteins (Figure 4a) follow first-order Fickian diffusive release. [23,24] Both BSA and insulin had an initial burst release of 11% and 22%, respectively, before controlled release was observed. A burst release was not observed for the larger IgG. The release rate of protein from the hydrogel correlated with protein molecular weight, with 77% of insulin released within the first 48 h while only 30% of IgG released over the course of 10 d. We attribute this protein size-dependent release effect to the mesh size of the hydrogel network. The glucose responsiveness of the hydrogels was also studied by monitoring the release of two model proteins, insulin and IgG from hydrogel network. It is expected that competitive binding to phenylboronic acid from freely diffusible glucose should disrupt the hydrogel network and accelerate the release of proteins from hydrogels. [25,26] The glucose levels chosen were 4 mg mL^{-1}, which is consistent with levels used to mimic hyperglycemia in diabetes patients, and 12 mg mL^{-1} as a high glucose concentration. Together, these buffers could enable probing of the effect of concentration on phenylboronic acid–diol binding equilibrium in the presence of very high glucose concentration. As the mesh size of the hydrogel was poorly selective to insulin, there was minimal effect of glucose on the release kinetics of insulin (Figure 4b). However, IgG, which did demonstrate size-selective release from the hydrogel, also exhibited glucose-dependent release kinetics (Figure 4c). 13% of IgG was released over 48 h in glucose-free PBS buffer, whereas 46% released in a buffer of 4 mg mL^{-1} glucose and 65% released in 12 mg mL^{-1} glucose. Over 120 h, 80% of the IgG released in the presence of 4 mg mL^{-1} glucose, while only 20% released in glucose-free conditions. Gradual dissociation of the IgG loaded gels exposed to glucose solutions is shown in Figure 4d. These results confirm glucose responsiveness of the PEG-FPBA hydrogels, and indicate glucose-responsive release for encapsulated proteins that are large enough such that release kinetics can be controlled by the mesh size of the hydrogel.

Injectable self-healing hydrogels may also have application as scaffolds for 3D support of cells. To evaluate cytocompatibility of these materials as 3D substrates, 3T3 fibroblasts were dispersed within the PEG-diol macromonomer prior to mixing with PEG-FPBA macromonomer for in situ hydrogel formation (10 w/v%). The presence of cells did not inhibit gel formation, and cells were dispersed homogenously within the hydrogel. To assess cytocompatibility, Live/Dead staining was performed after cells had been cultured within the material for 72 h. The majority of cells encapsulated within PEG-FPBA gel remained viable, indicating minimal cytotoxicity in response to the material or its in situ cross-linking mechanism (Figure 4e,f). However, when cells were dispersed in PEG-FPBA hydrogels and subsequently extruded through a syringe (21 gauge), cell viability was not preserved, which is attributed to the high shear rates necessary to induce shear-thinning in the gel. Moreover, the toxicity of hydrogel degradation products was evaluated using gel extracts (Figure S2, Supporting Information). Gel extracts were obtained by incubating hydrogels (10 w/v%) in 1 mL of cell culture media for 72 h at 37 °C. To assess the toxicity of the gel degradation

products, 3T3 fibroblast cells were then cultured in gel extract media for 24 h and toxicity was quantified using an MTT assay. No significant cytotoxicity was observed in response to gel extracts, as cell number was in excess of 85% compared to untreated controls. In addition to MTT quantification, viable cells were also visualized using Live/Dead staining, which confirmed that the vast majority of cells remained viable (Figure S2, Supporting Information).

To evaluate tissue biocompatibility, hydrogels prepared from PEG-FPBA were applied by transcutaneous injection via extrusion from an 18 G syringe needle. The material formed a visible gel mass in the subcutaneous space. At serial time points following injection, the hydrogel and its surrounding implantation bed were harvested and processed for qualitative histological analysis (Figure 5). At 3 d following injection, only the outer margins of the hydrogel had been infiltrated by immune cells, primarily monocytes. There was also evidence of a mild inflammatory response in the peri-implant tissue. By 7 d, the number of infiltrating cells had increased, as had the extent to which the material had been infiltrated, though the center of the scaffold remained uninfiltrated by cells. At this time, monocytes were still the primary cell population present. There was again evidence of mild infiltration and some tissue damage in the peri-implant tissue. By 14 d, the gel was completely infiltrated by a large number of immune cells, with the appearance of an appreciable inflammatory response. At this time, the presence of monocytes was reduced, and most infiltrating cells were macrophages with a large number of multinucleated giant cells also present. There was evidence of both inflammation and tissue damage in the peri-implant tissue. One month following injection of the hydrogel, the material had been replaced with a vascularized connective tissue, suggesting cell-mediated material clearance. The number of infiltrating inflammatory cells was dramatically reduced. There was also no sign of inflammation or tissue damage in the peri-implant tissue, with the entire implant site appearing to have healed by this time. Overall, the kinetics and characteristics of the tissue reaction to the implanted hydrogel were consistent with those of a typical foreign body reaction to an implanted material, and no chronic effects were noted. [27]

In summary, we have designed and synthesized a library of self-healing hydrogels based on dynamic covalent bond formation between phenylboronic acid and *cis*-diol modified PEG macromonomers. The effect of pH on the gelation behavior was investigated to formulate hydrogels with highly tunable mechanical properties. The nature of this dynamic covalent chemistry enables shear-thinning delivery of the gels via syringe, followed by rapid structural recovery (self-healing). These gels also exhibit size-dependent controlled release of proteins encapsulated within the network as well as glucose-responsive release of larger proteins. The materials are cytocompatible in vitro, and the tissue reaction in vivo was consistent with a typical foreign body reaction with no chronic inflammation. These injectable, self-healing hydrogels could have many applications, such as 3D cell culture substrates for tissue engineering as well as controlled release of macromolecule for drug delivery applications.

Supplementary Material

Refer to Web version on PubMed Central for supplementary material.

Acknowledgments

This work was supported by a grant from the Leona M. and Harry B. Helmsley Charitable Trust (Award No. 2014PG-T1D002). M.J.W. is extremely grateful for the financial support from the National Institutes of Health through Ruth L. Kirschstein National Research Service Award No. F32DK101335. E.A.A. is extremely grateful for financial support through a Wellcome Trust-MIT Postdoctoral Fellowship. The authors acknowledge Timothy M. O'Shea for helpful discussions related to protein release studies. The animal studies were approved by the Institutional Animal Care and Use Committee of the Massachusetts Institute of Technology.

References

1. Vermonden T, Censi R, Hennik WE. Chem Rev. 2012; 112:2853. [PubMed: 22360637]
2. Peppas NA, Hilt JZ, Khademhosseini A, Langer R. Adv Mater. 2006; 18:1345.
3. Malda J, Visser J, Melchels FP, Jungst T, Hennink WE, Dhert WJA, Groll J, Hutmacher DW. Adv Mater. 2013; 25:5011. [PubMed: 24038336]
4. Li L, Yan B, Yang J, Chen L, Zeng H. Adv Mater. 2015; 27:1294. [PubMed: 25581601]
5. You J, Auguste DT. Langmuir. 2010; 26:4607. [PubMed: 20199077]
6. Rowan SJ, Cantrill SJ, Cousins GRL, Sanders JKM, Stoddart JF. Angew Chem, Int Ed. 2002; 41:898.
7. McKinnon DD, Domaille DW, Cha JN, Anseth KS. Chem Mater. 2014; 26:2382.
8. Smeets NMB, Bakaic E, Patenaude M, Hoare T. Chem Commun. 2014; 50:3306.
9. Appel EA, Dyson J, Barrio JD, Walsh Z, Scherman OA. Angew Chem, Int Ed. 2012; 51:4185.
10. Cambre JN, Sumerlin BS. Polymer. 2011; 52:4631.
11. Ma R, Shi L. Polym Chem. 2014; 5:1503.
12. Kotsuchibashi Y, Agustin RVC, Lu JY, Hall DG, Narain R. ACS Macro Lett. 2013; 2:260.
13. Bapat AP, Roy D, Ray JG, Savin DA, Sumerlin BS. J Am Chem Soc. 2011; 133:19832. [PubMed: 22103352]
14. He L, Fullenkamp DE, Rivera JG, Messersmith PB. Chem Commun. 2011; 47:7497.
15. Roy D, Cambre JN, Sumerlin BS. Chem Commun. 2009:2106.
16. Matsumoto A, Ishii T, Nishida J, Matsumoto H, Kataoka K, Miyahara Y. Angew Chem, Int Ed. 2012; 51:2124.
17. Matsumoto A, Ikeda S, Harada A, Kataoka K. Biomacromolecules. 2003; 4:1410. [PubMed: 12959613]
18. Piest, M. PhD Thesis. University of Twente; Enschede, The Netherlands: 2011.
19. Appel EA, Biedermann F, Rauwald U, Jones ST, Zayed JM, Scherman OA. J Am Chem Soc. 2010; 132:14251. [PubMed: 20845973]
20. Piest M, Zhang X, Trinidad J, Engbersen JFJ. Soft Matter. 2011; 7:11111.
21. McKinnon DD, Domaille DW, Cha JN, Anseth KS. Adv Mater. 2014; 26:865. [PubMed: 24127293]
22. Roberts MC, Hanson MC, Massey AP, Karren EA, Kiser PF. Adv Mater. 2007; 19:2503.
23. Ritger PL, Peppas NA. J Controlled Release. 1987; 5:37.
24. Ma D, Zhang LM, Xie X, Liu T, Xie MQ. J Colloid Interface Sci. 2011; 359:399. [PubMed: 21536304]
25. Yang T, Ji R, Deng XX, Du FS, Li ZC. Soft Matter. 2014; 10:2671. [PubMed: 24647364]
26. Bratlie KM, York RL, Invernale MA, Langer R, Anderson DG. Adv Healthcare Mater. 2012; 1:267.
27. Anderson JM, Rodriguez A, Chang DT. Semin Immunol. 2008; 20:86. [PubMed: 18162407]

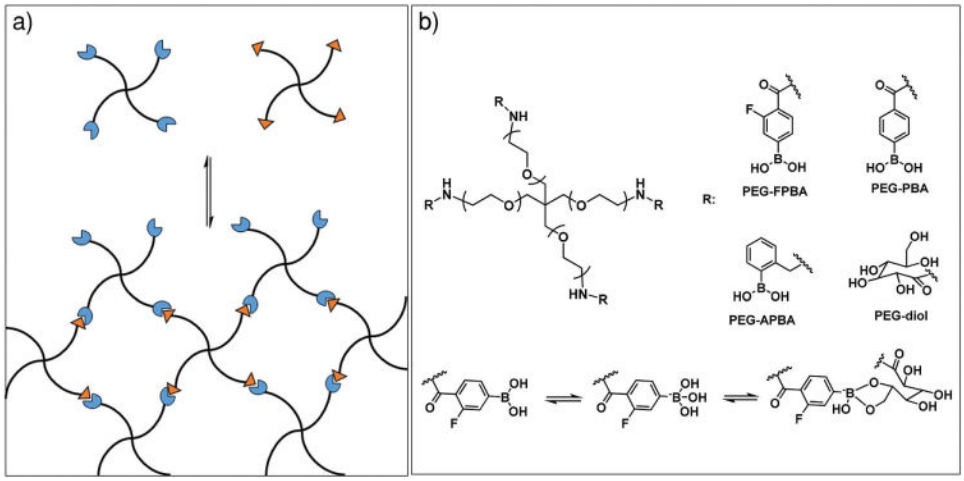

Figure 1.

a) Schematic depicting hydrogel formation between four-arm phenylboronic acid–containing PEG macromonomers and diol-containing PEG macromonomer. b) Chemical structures of PEG-phenylboronic acid macromonomers and PEG-diol, and the representative mechanism of phenylboronic acid-*cis*-diol binding.

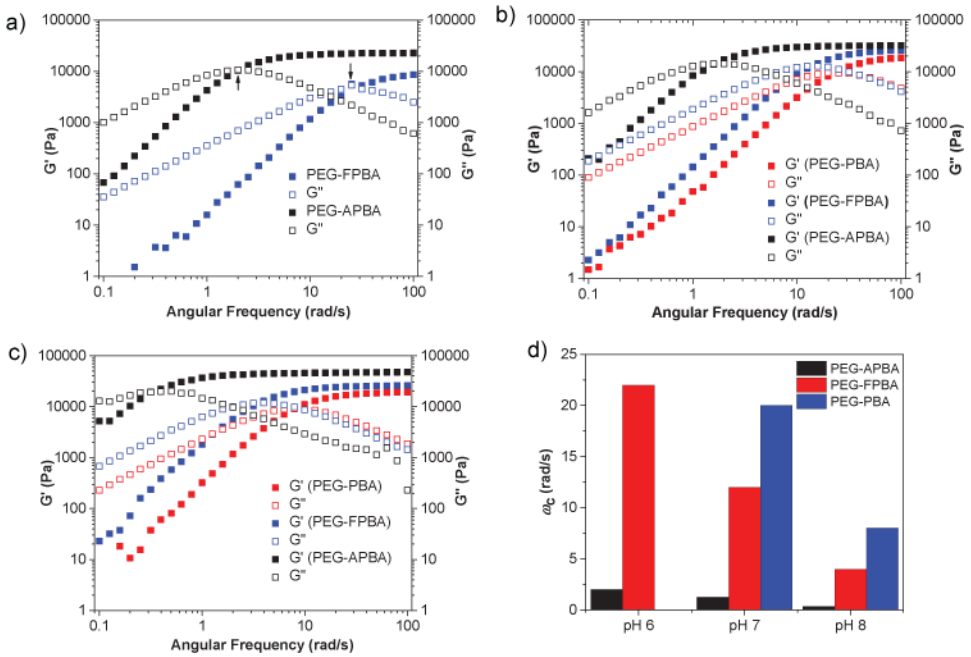

Figure 2.

Dynamic oscillatory frequency sweeps performed at 37 °C of 10 w/v% hydrogels formed at a) pH 6, b) pH 7, and c) pH 8. d) The crossover frequencies (ω_c) obtained from frequency sweeps at each pH value for hydrogels. Arrows in (a) denote representative crossover frequencies.

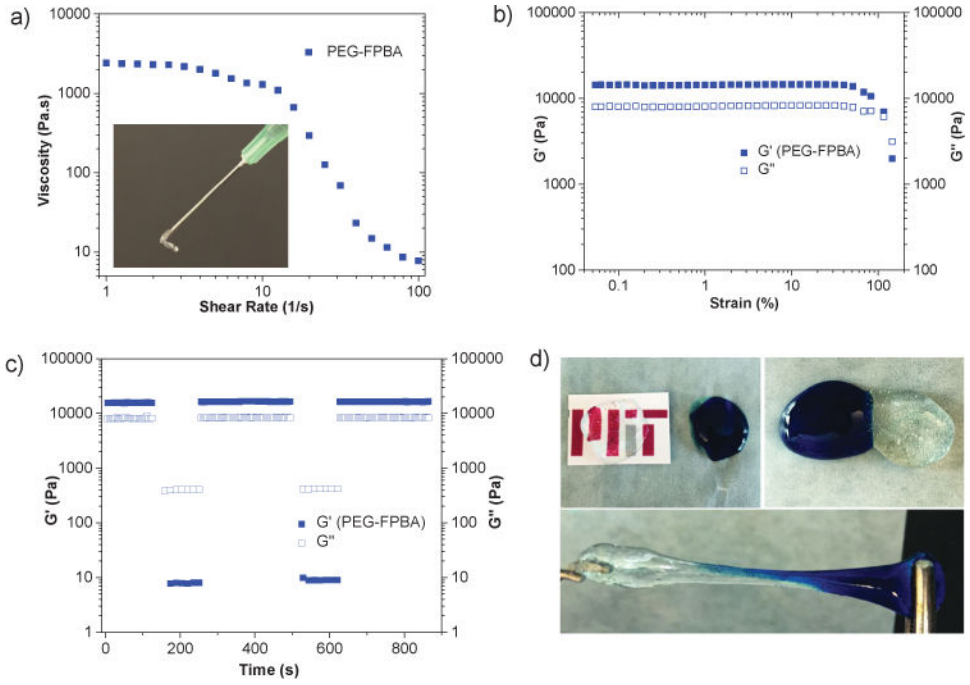

Figure 3.

a) Viscosity and shear-thinning behavior of 10 w/v% PEG-FPBA gel. The inset shows that gel is injectable through a conventional syringe using a 21 G needle. b) Strain amplitude sweep. c) Step–strain measurements of 10 w/v% PEG-FPBA gel formed at pH 7. d) Demonstration of the self-healing properties of 10 w/v% PEG-FPBA gel, formed at pH 7, in fusing two hydrogel pieces. Gel was prepared in the presence of methylene blue for observation.

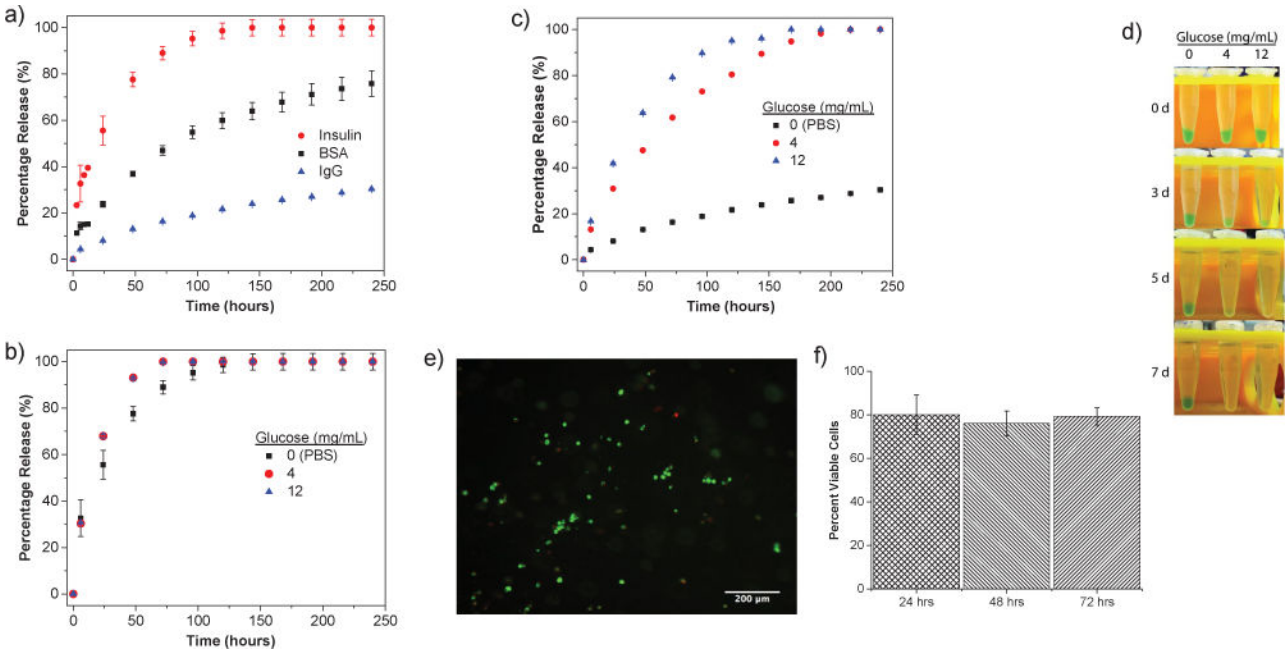

Figure 4.

Release profiles of proteins from 10 w/v% PEG-FPBA hydrogels formed at pH 7. a) Release profiles in 1× PBS buffer. Release of b) insulin and c) IgG at different glucose concentrations. d) Pictures of IgG loaded 10 w/v% PEG-FPBA gels incubated in different glucose concentrations over 7 d. e) LIVE/DEAD assay image of cells encapsulated within 10 w/v% PEG-FBA hydrogels for 72 h. (Scale bar: 200 µm, green: live, red: dead.) f) Cell viability quantified at different time points (24–72 h).

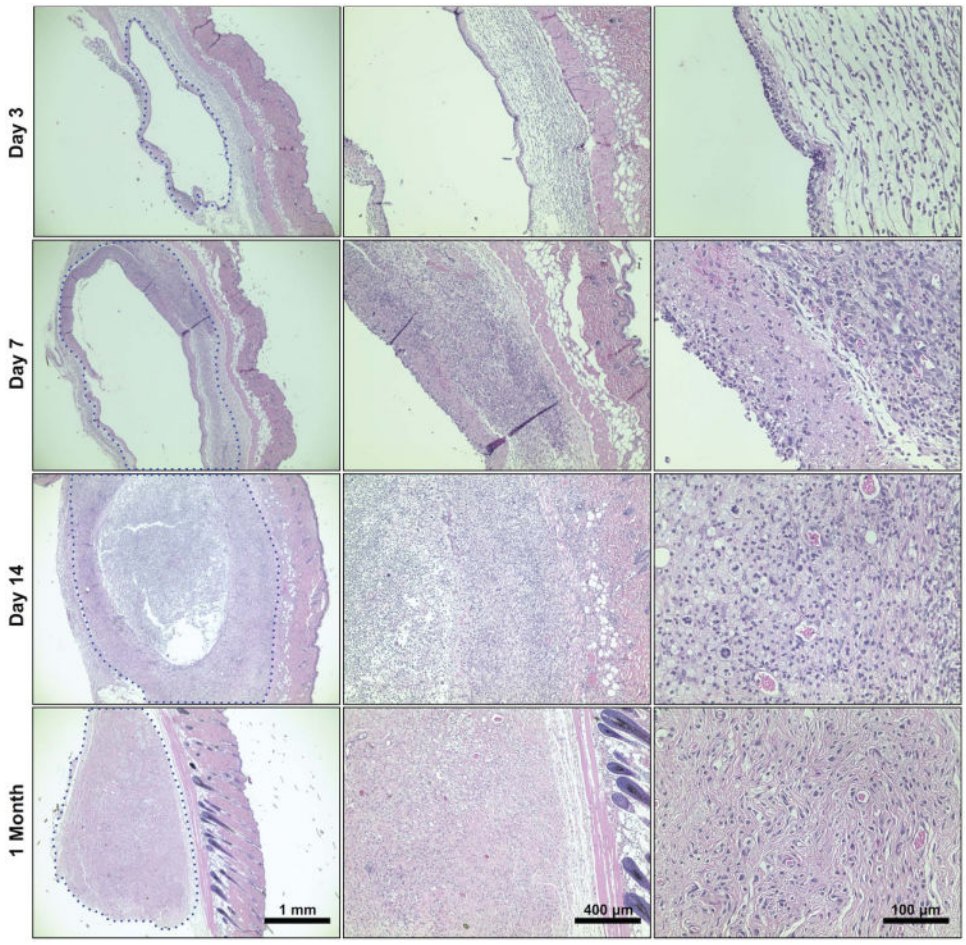

Figure 5.

Histological images (H&E staining) of 10 w/v% PEG-FPBA gels injected subcutaneously and harvested at 3 d, 7 d, 14 d, and 1 month following injection. Shown is a cross section of skin (oriented to the right in all images) with the underlying material. In the lowest magnification images (left column), the approximate location of the margins of material is noted with a blue dotted outline. Intermediate magnification images (center column) show the material–tissue interface, while high magnification images (right column) show infiltrating cells within the material. Scale bars shown apply to entire column. A low magnification image (first column) shows the entire implant bed and peri-implant tissue, an intermediate magnification (middle column) shows the cell–material interface, and a high magnification image (right column) shows the specific cells present in the implant–tissue interface.